

## Topics

Characterizing galaxy structure

Surface brightness

Structural parameters

Disks

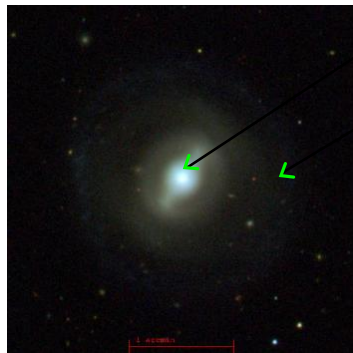
Ellipticals

Bulges

1

1

## Surface Brightness:



High surface brightness

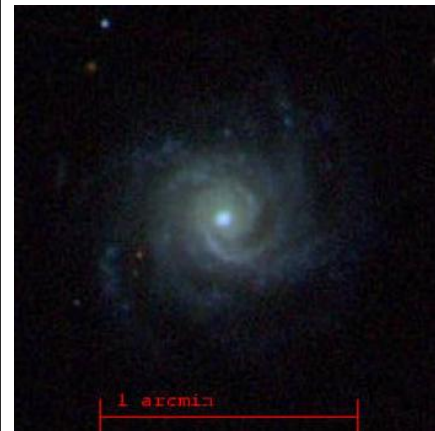
Low surface brightness

$I, \Sigma$  = "Intensity" or "Surface Brightness"  
= Flux / Angular Area ( $\text{ergs/s/cm}^2/\text{arcsec}^2$ )  
= Luminosity / Area  $(L_\odot/\text{pc}^2)$

3

3

## Quantifying Galaxy Images:



How do you turn the pretty pictures into something quantitative?

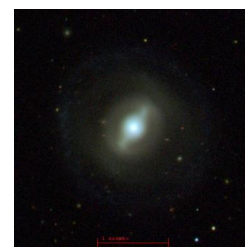
"Surface Photometry": Quantify surface brightness as a function of position.

2

Why? Surface photometry reveals the distribution of stellar mass.

2

## Surface Brightness vs Surface Density



$$\text{Surface density} = \Sigma \times \Upsilon_\star$$

surface density:  $M_\odot/\text{pc}^2$

stellar mass-to-light ratio:  $\Upsilon$  in  $M_\odot/L_\odot$

$I, \Sigma$  = "Intensity" or "Surface Brightness"  
= Flux / Angular Area ( $\text{ergs/s/cm}^2/\text{arcsec}^2$ )  
= Luminosity / Area  $(L_\odot/\text{pc}^2)$

4

4

## Surface Brightness vs Distance

1. Approximately constant with distance nearby:

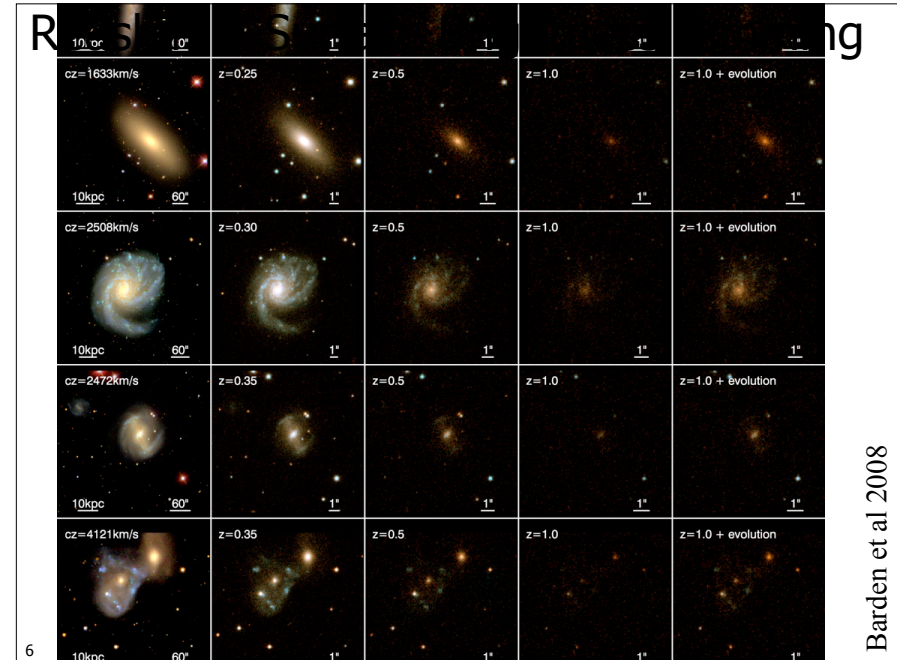
$$\frac{\text{Flux}}{\text{AngularArea}} = \frac{L/4\pi D_L^2}{\text{Area}/D_A^2} \propto \frac{L}{\text{Area}} = \text{constant}$$

2. Falls off rapidly at high redshift:

$$(D_A/D_L)^2 = (1+z)^{-4}$$

5

5



6

Barden et al 2008

## Surface Brightness Units

Usually converted to the world's worst astronomical units:

$\mu$  = the magnitude of a 1 arcsec<sup>2</sup> patch  
= magnitudes / arcsecond<sup>2</sup>  
= constant - 2.5 log<sub>10</sub> Σ

7

7

## Typical Surface Brightness Values

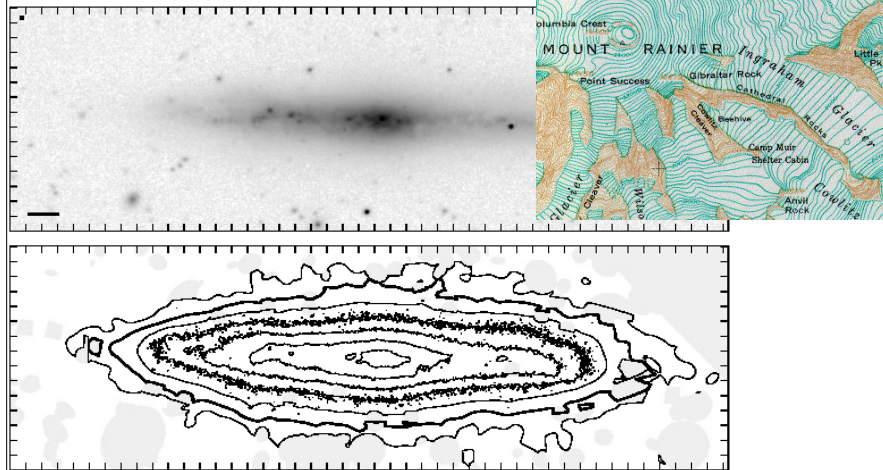
$\mu$  = the magnitude of a 1 arcsec<sup>2</sup> patch  
= magnitudes / arcsecond<sup>2</sup>  
= constant - 2.5 log<sub>10</sub> Σ

$\mu_{\text{sky}} \sim 22 \text{ B-mag/sqr-''}$   
 $\mu_0(\text{spiral disks}) \sim 21.7 \text{ B-mag/sqr''}$   
(“Freeman Value” 1970)  
 $\mu_{\text{lim, shallow}} \sim 25 \text{ B-mag/sqr''}$   
 $\mu_{\text{lim, deep}} \sim 28-29 \text{ B-mag/sqr''}$   
 $\mu_{\text{Holmberg}} \sim 26.5 \text{ B-mag/sqr''}$

8 Note: Subscript “0” means either “central” or “at the present day”

8

Isophotes: lines of constant surface brightness



9

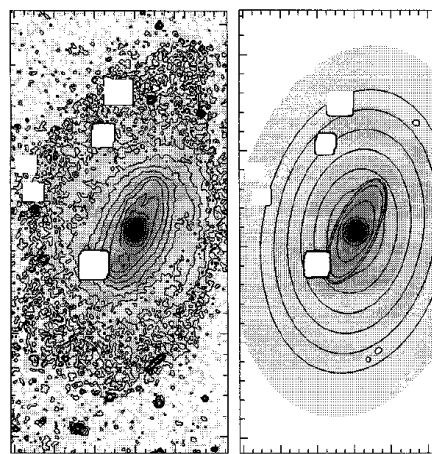
Measuring Surface Brightness =  
“Surface Photometry”

Approximate isophotes as:

A sum of models of multiple components (disk+bulge+bar)

or

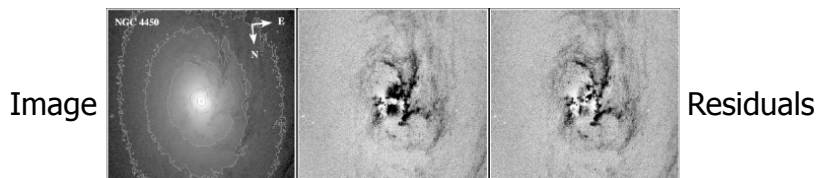
Nested quasi-ellipses with varying position angles & ellipticities



See “Galfit” by Peng et al 2002,2010 or Gim2D by Simard

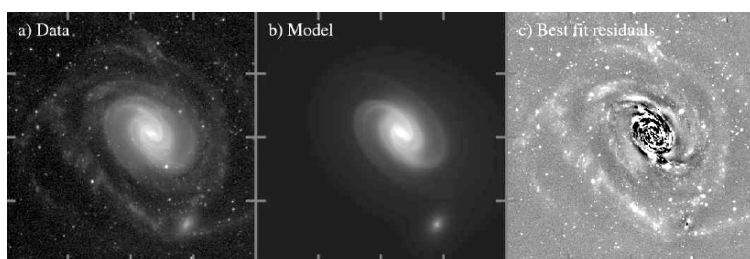
10

Example of model decomposition



Image

Residuals

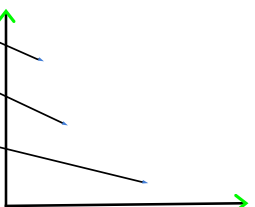
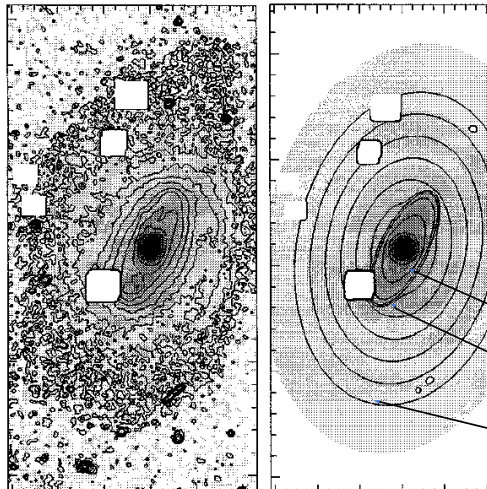


Galfit: Peng et al 2002,2010

11

“Surface Brightness Profile”

Surface brightness vs. major axis length.

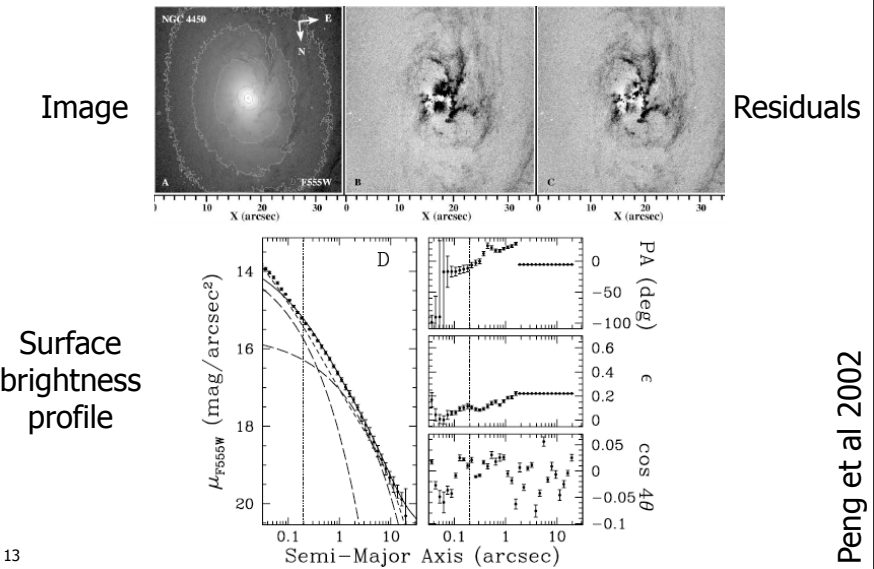


Use elliptical fits or models

12

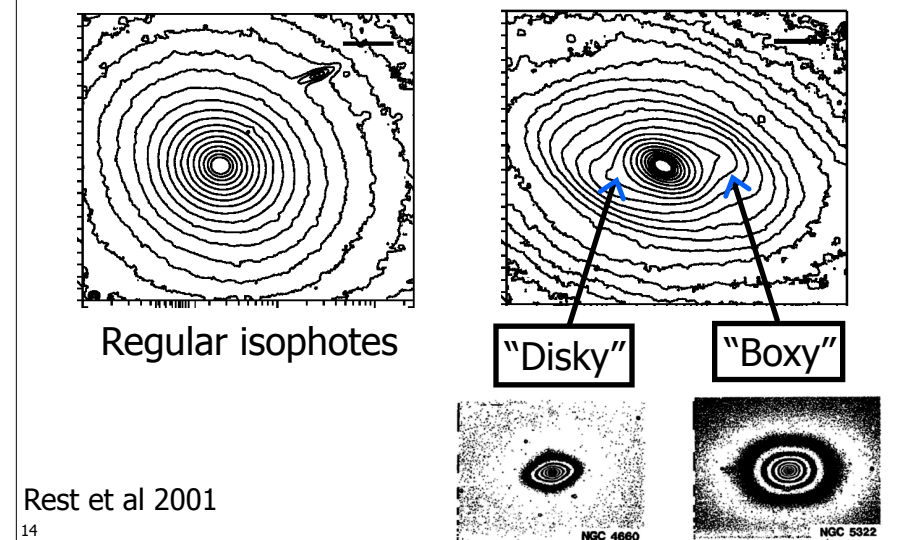
12

## Example of model decomposition



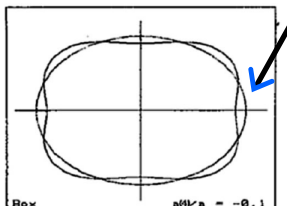
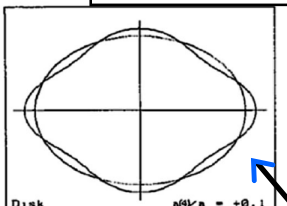
13

## Often necessary to characterize deviations from ellipticity



14

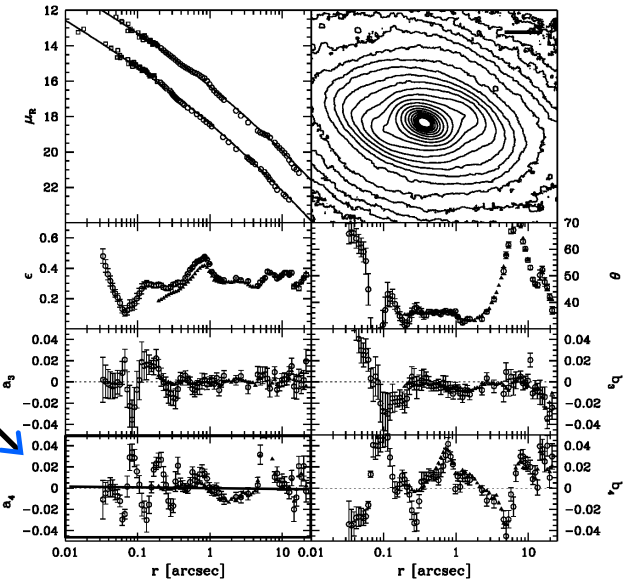
$$\frac{\delta r(\theta)}{r(\theta)} = \sum_{n=3}^4 [a_n \sin(n\theta) + b_n \cos(n\theta)]$$



$a_4 < 0$  : boxy isophotes  
 $a_4 > 0$  : disky isophotes

## Example of Non-zero $a_4$ components...

Alternating  
between  
positive and  
negative as  
it goes from  
disky to  
boxy



## Surface Brightness vs Luminosity:

$$L(< r) = \int_0^r \Sigma(r) 2\pi r dr$$

Total Luminosity:

$$L_{tot} = L(< r \rightarrow \infty) = 2\pi\Sigma_0 h_r^2$$

For an exponential disk with scale length  $h_r$ , central sb  $\Sigma_0$

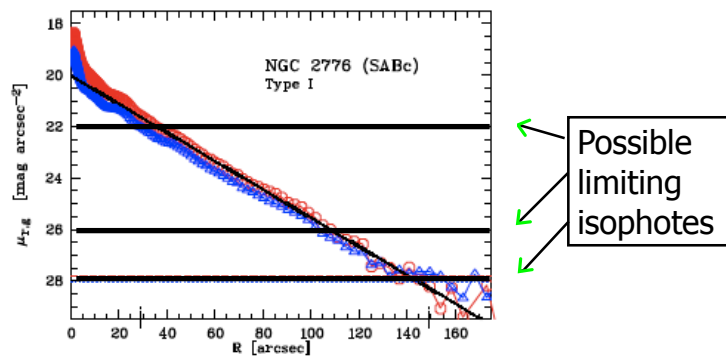
"Half-light radius":  $r_{1/2}$  or  $r_e$

$$L(< r_{1/2}) = \int_0^{r_{1/2}} \Sigma(r) 2\pi r dr = \frac{1}{2} \int_0^{\infty} \Sigma(r) 2\pi r dr$$

17

17

## Measured Luminosity $\neq$ Total Luminosity!



Can only measure light that falls above the "limiting isophote"  
(set by noise+systematics of background)

19

19

## Galaxy Luminosity

More complicated than stars.

Must define area of flux measurement

Fixed aperture (3", 1', etc)

Scaled aperture (4 scale lengths, etc)

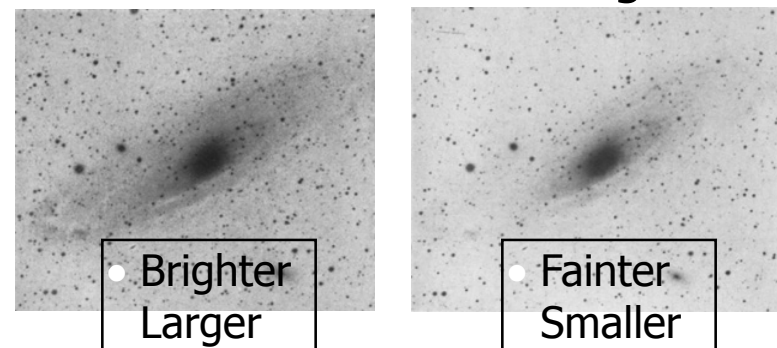
Isophotal aperture (flux within  $m_{lim}$ )

Differences between these can be substantial and important.

18

18

## Luminosity & size affected by sky noise relative to surface brightness

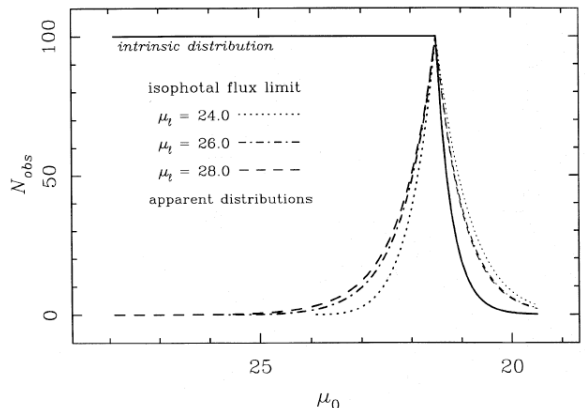


"Selection Bias": lower surface brightness galaxies (LSBs) are underrepresented in catalogs of galaxies (defined as larger than or brighter than some limit).

20

20

## Bias against low surface brightness disks



This apparent peak was first noted by Freeman (1970), and is known as the "Freeman Law" or "Freeman surface brightness" of 21.7 B-mag/sqr-arcsec. Disney (1976) pointed out that the apparent constancy of disk surface brightnesses could instead be a "selection effect"

21

## Structure of Spiral Disks

Exponential

Possibly truncated

22

## "Exponential Disks"

### Spirals & Dwarfs: "Exponential Disks"

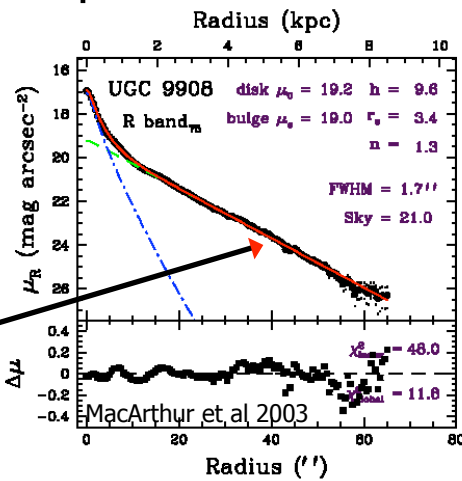
$$\Sigma_{\text{disk}}(r) = \Sigma_0 e^{-r/h}$$

Straight line when plotted logarithmically

$$\mu(r) = C - 2.5 \log_{10} \Sigma(r)$$

"Exponential Disk with Scale length  $h_r$  and central surface brightness  $\Sigma_0$ "

23



23

## "Exponential Disks"

$$\Sigma_{\text{disk}}(r) = \Sigma_0 e^{-r/h}$$

Or, in magnitudes per sqr-arcsec:

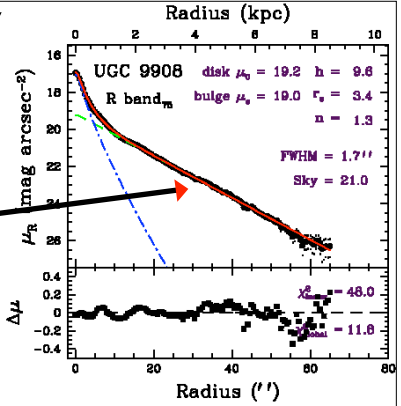
$$\mu_{\text{disk}}(r) = \mu_0 + 1.086r/h$$

Intercept = Central surface brightness

Slope =  $1.086/h$

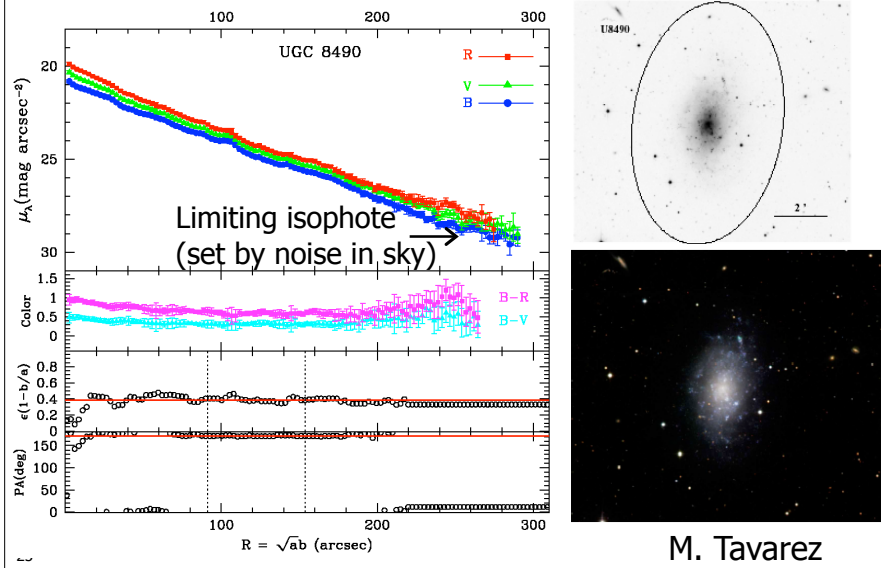
[Subscript "0" = "central"]

24



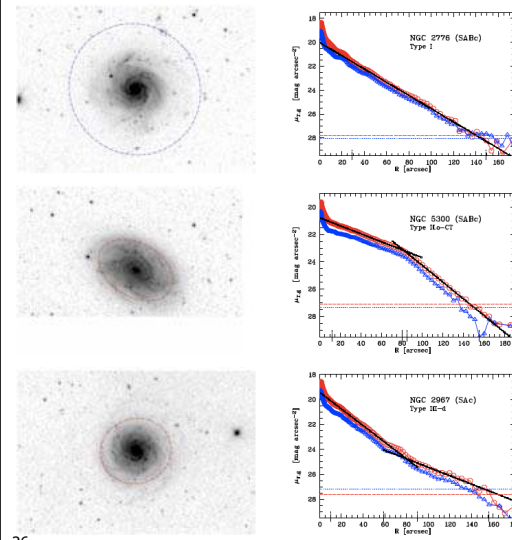
24

## Example of a “pure” exponential disk



25

## Complex Profiles in Face-On Disks



Unbroken:  
10%

“Truncated”:  
60%

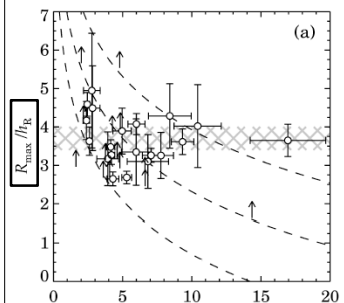
Upbending:  
30%

Pohlen & Trujillo 2006

26

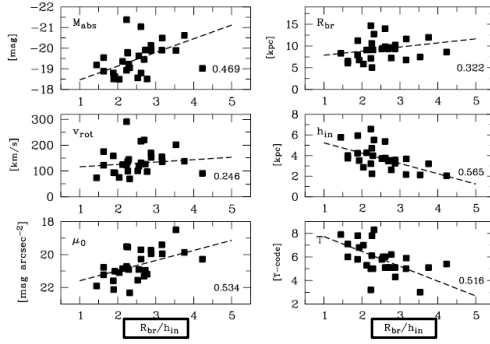
## Disk Breaks at $\sim 2\text{-}4h_r$

### Edge-on



Kregel & van der Kruit 2004

### Face-on



Warp? Star formation threshold +  
Resonant scattering?

27

27

## Structure of Ellipticals

3D shapes

DeVaucouleurs ( $r^{-1/4}$ )

Sersic profiles ( $r^{-1/n}$ )

Profile depends on mass

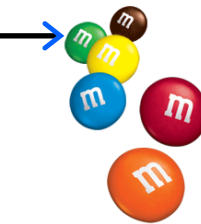
28

28

# 3-Dimensional Shapes of Ellipticals



Oblate ( $a = b > c$ )



Prolate ( $a > b = c$ )



Triaxial ( $a \neq b \neq c$ )

$a, b, c$  are the long, intermediate, and short axis lengths ( $a \geq b \geq c > 0$ )

Triaxiality parameter

$$\epsilon_1 = 1 - \frac{c}{a}, \quad \epsilon_2 = 1 - \frac{b}{a}$$

29

$$T = \frac{a^2 - b^2}{a^2 - c^2} = \frac{\epsilon_2(2 - \epsilon_2)}{\epsilon_1(2 - \epsilon_1)}$$

29

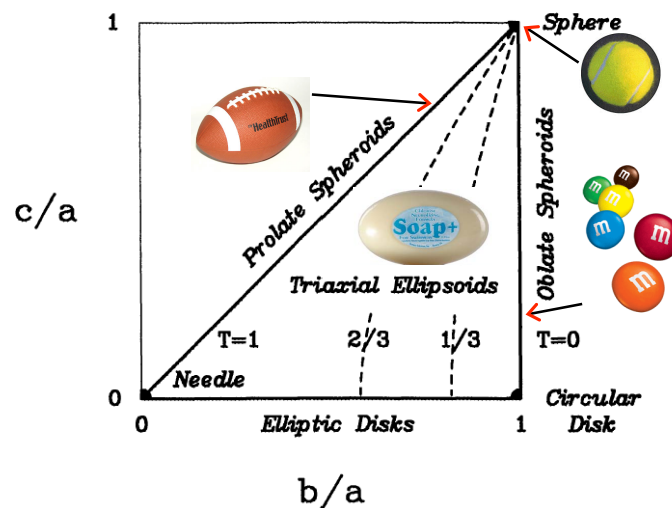


Figure 1 Ellipsoid Land: the plane of all possible axial ratios  $b/a$  and  $c/a$  for triaxial ellipsoids. The limiting cases with more symmetry are indicated. The dashed lines are curves of constant triaxiality  $T$  (see Section 3.4). Oblate spheroids have  $T = 0$ , prolate spheroids have  $T = 1$ .

30

## What do we know about the 3-d shapes of ellipticals?

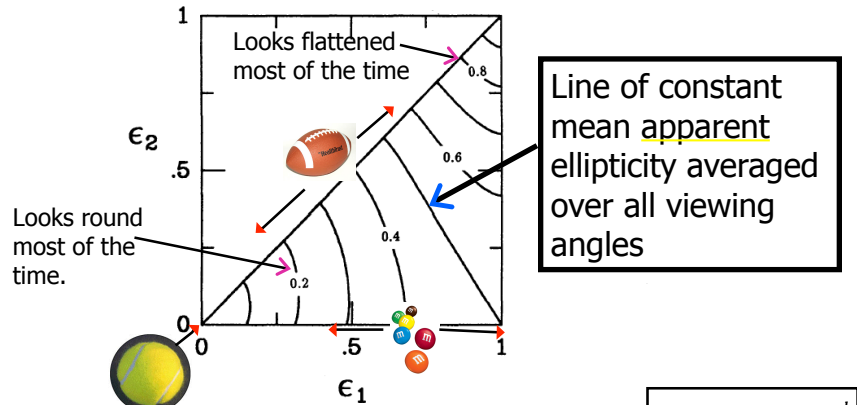
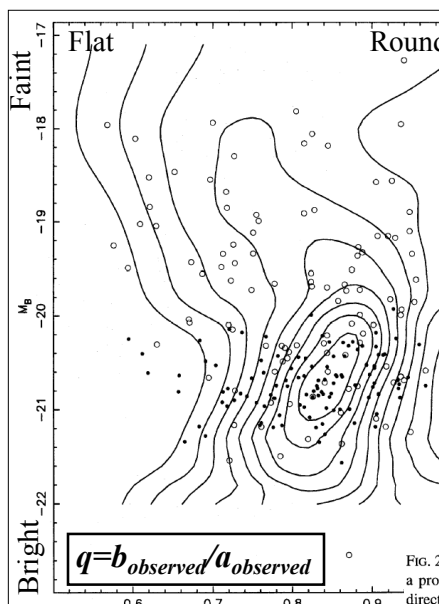


FIG. 3.—Contours of constant mean apparent ellipticity  $\langle \epsilon \rangle$  in the plane of all shapes;  $\langle \epsilon \rangle$  is the apparent ellipticity averaged over all possible viewing angles. Contours are drawn at intervals of 0.1. For low  $\epsilon_1$ ,  $\langle \epsilon \rangle$  is only weakly dependent on  $\epsilon_2$ .

Franx et al 1991

31



32 Tremblay & Merritt 1996

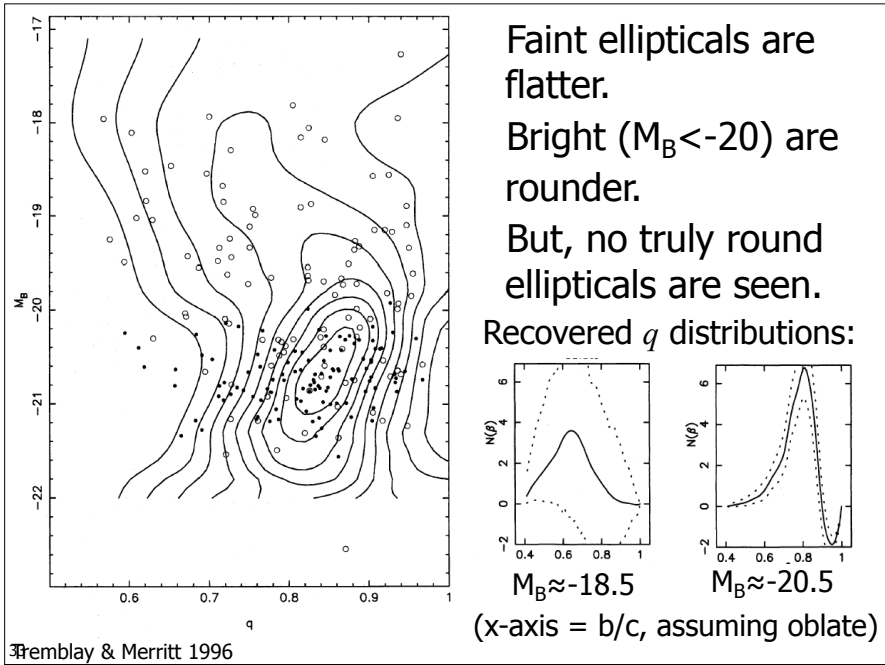
Assume a triaxiality  $T$ , and do nasty, nasty math to invert the observed distribution of  $q = b/a$ .

Observed distribution, and smoothed estimate of the observed distribution

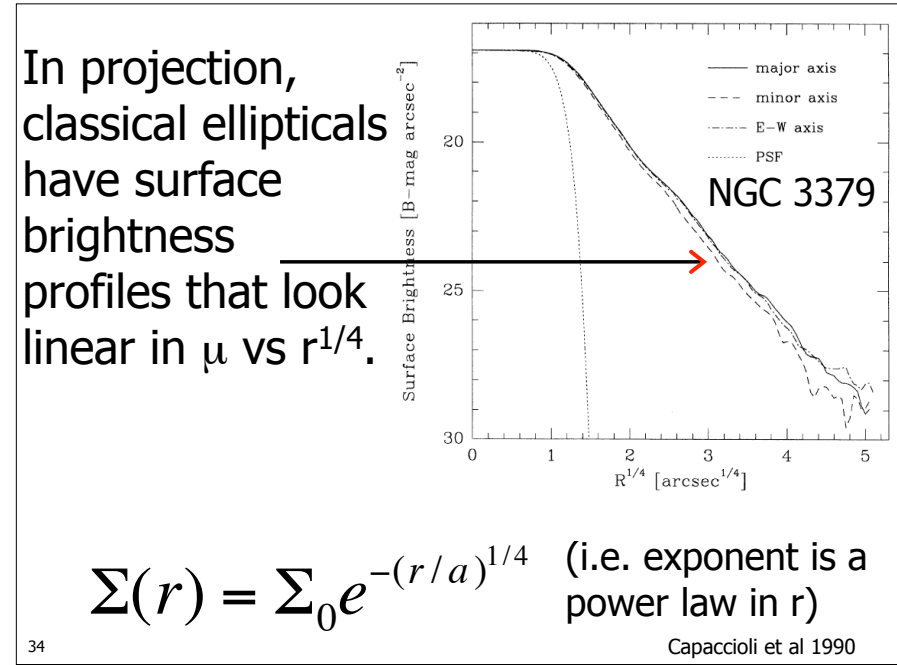
Fig. 2. Estimate of  $f(q, M_B)$  for the 220 galaxies in our sample, obtained via a product-kernel technique with different window widths in the  $q$  and  $M_B$  directions. The function  $f$  has been normalized at every  $M_B$  to give unit area when integrated along  $q$ . Circles are galaxies in the Djorgovski—Ryden sample; dots are from the Lauer—Postman sample. The six galaxies in both samples are indicated by circles. Contours are separated by 0.5 in  $f$ .

32

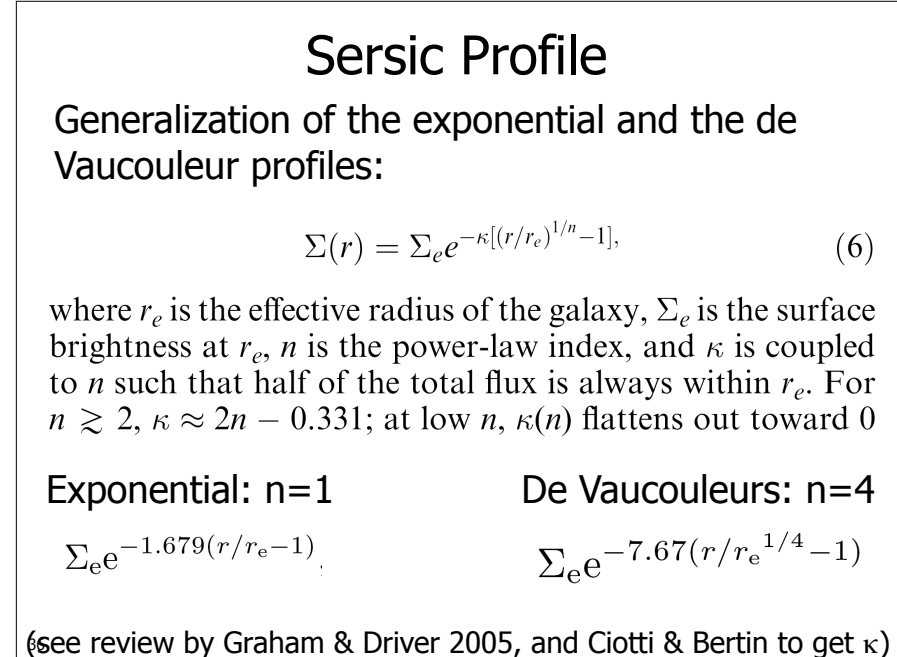
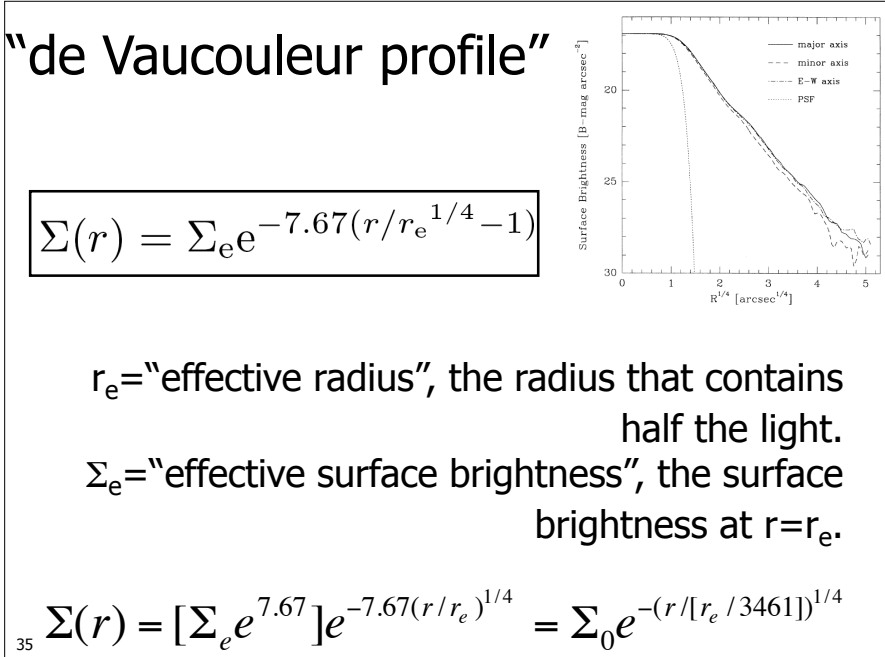
De Zeeuw & Franx 1991



33

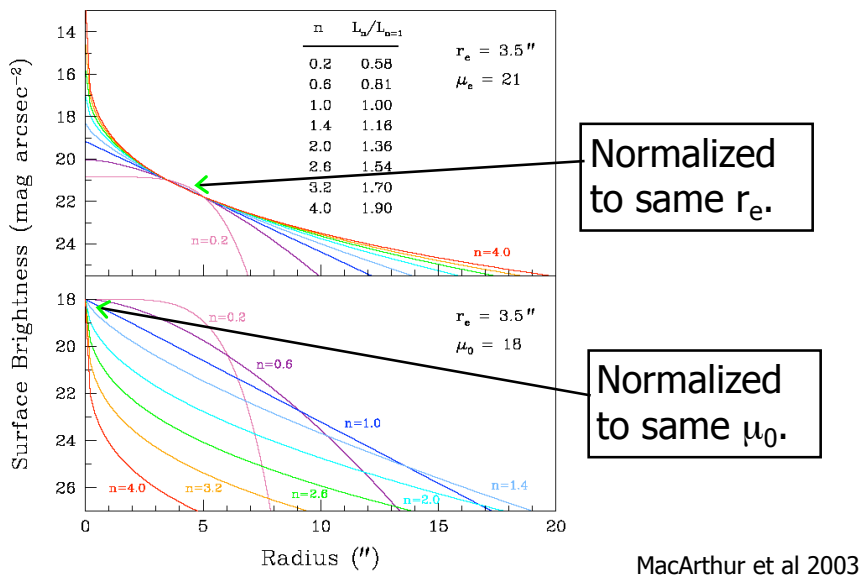


34

35  
36

35

Sersic profiles:  $\Sigma(r) = \Sigma_e e^{-\kappa[(r/r_e)^{1/n}-1]}$



37

For ellipticals,  
the extra  
freedom of the  
Sersic profile  
improves the fit  
of the model to  
data.

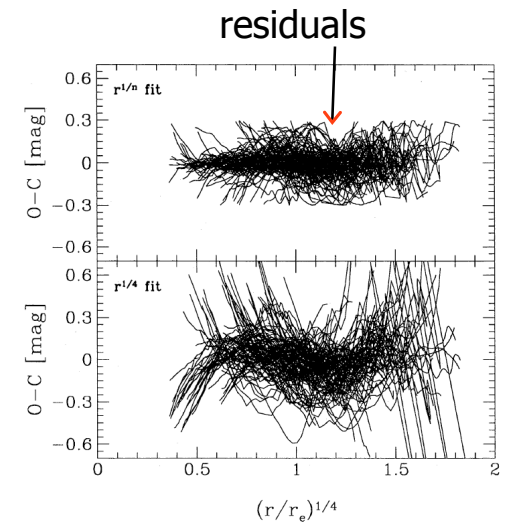
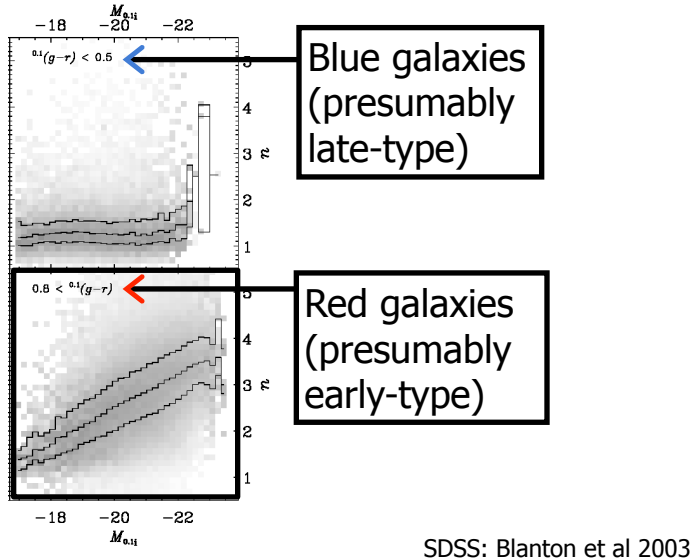


Figure 2. Radial run of the (O-C) residuals (in magnitudes) for the fit of the  $B$  light profiles of our Virgo galaxies (Table 2) with the  $r^{1/n}$  law (upper panel) and with the de Vaucouleurs law (lower panel); the abscissa is the reduced galactocentric distance  $(r/r_e)^{1/4}$ .

38 Caon et al 1993

38

Smaller ellipticals = smaller Sersic  $n$



39

39

## Structure of Bulges

Tricky!

Profile depends on mass.

More massive bulges are more deVaucouleurs.

Late-type galaxy bulges may be “pseudobulges”, built from disk material

40

40

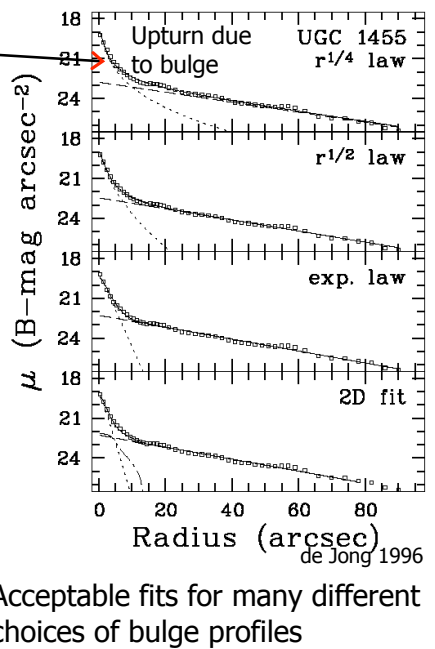
# Surface Photometry of Bulges

Hard to separate the bulge from the disk.

Can fit 1-d profiles or 2-d profiles.

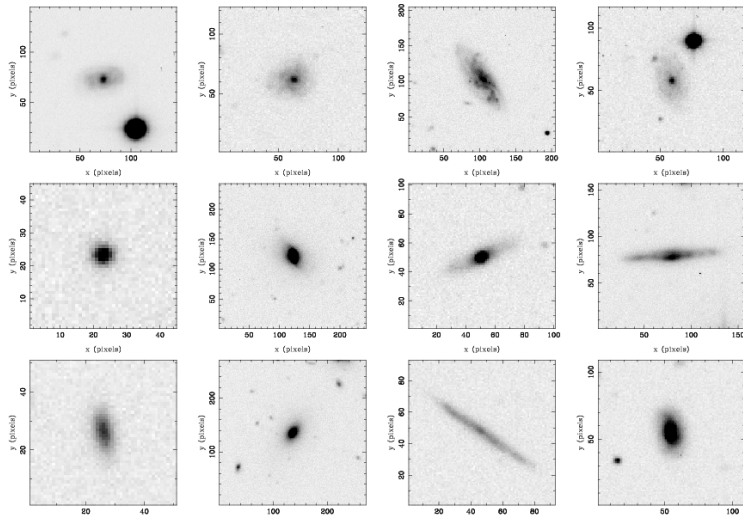
Latter is more robust.

41



41

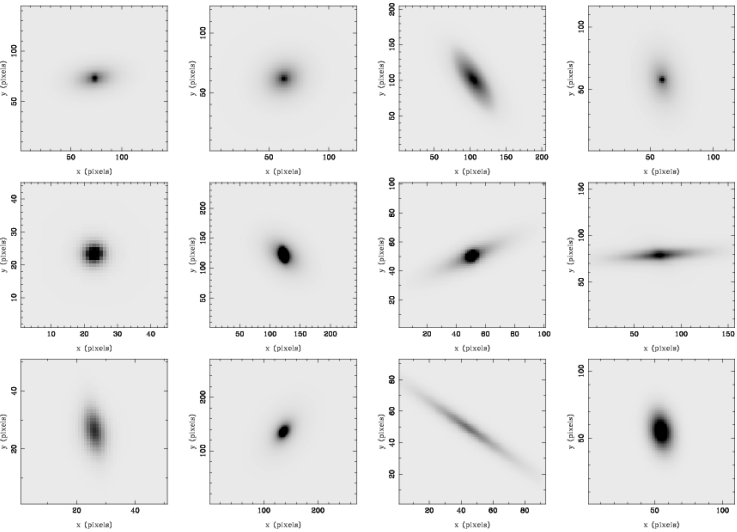
## Data



Millennium Galaxy Catalog: Allen et al 2006

42

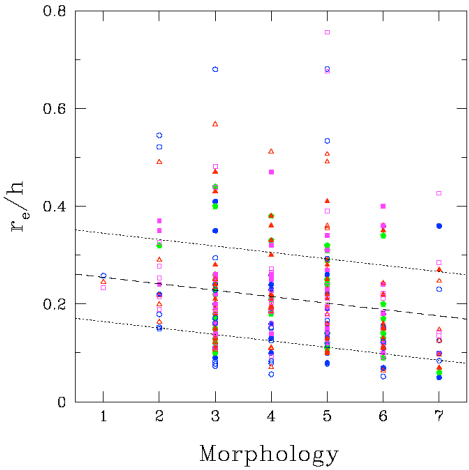
## Model



43

## Bulge sizes vs Disk sizes

Typically,  
 $r_e \sim h/5$



MacArthur et al 2003

Fig. 21.— Distribution of  $r_e/h$  with Hubble types for our Type-I galaxies and those of Graham (2001). Symbols and colors are as in Fig. 20. The dashed line describes the fit  $\langle r_e/h \rangle = 0.20 - 0.013(T - 5)$  with  $1\sigma = 0.09$  errors (dotted lines) based on our data only.

43

44

## Bulge Profiles:

$$\Sigma(r) = \Sigma_e e^{-\kappa[(r/r_e)^{1/n} - 1]}$$

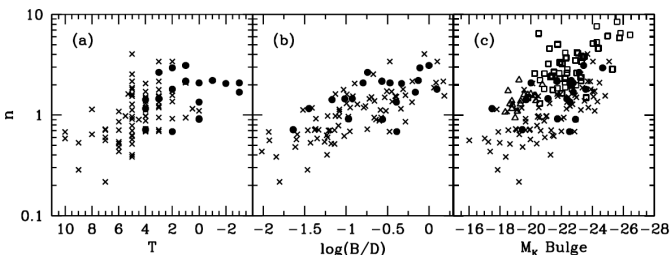
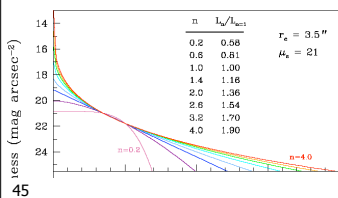


FIG. 6.— The bulge Sérsic index  $n$  is plotted against: (a) the revised morphological type index  $T$  from the RC3; (b)  $B/D$  derived from the best-fit parameters; and (c) the bulge  $K$ -band absolute magnitude derived from  $B/D$  and the galaxy  $K$ -band absolute magnitude, corrected for Galactic extinction, cosmological dimming and  $K$ -correction. Filled circles: bulges, this work. Crosses: bulges from the de Jong & van der Kruit (1994) sample, as analyzed by Graham (2001a, 2003). Triangles: Coma dwarf ellipticals from Graham & Guzman (2003). Squares: Virgo ellipticals from Caon et al. (1993).

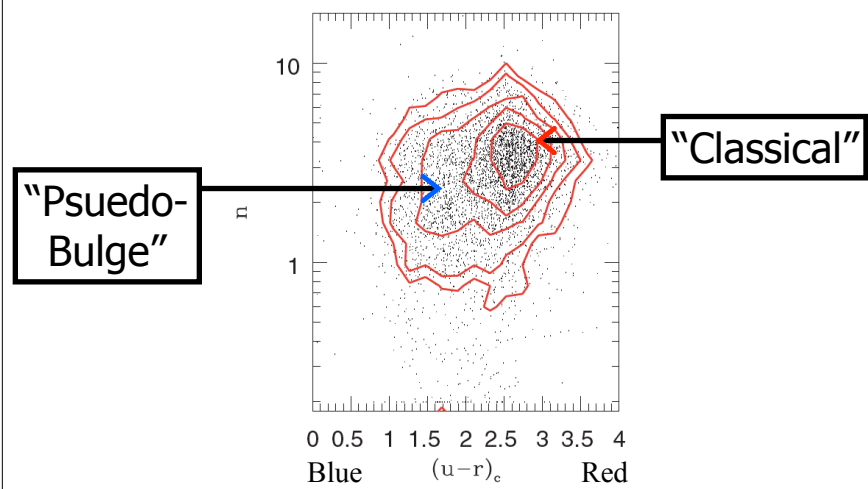


Late-type galaxy bulges are more exponential ( $n=1$ ) than deVaucouleurs ( $n=4$ )

Balcells et al 2003, based on NICMOS data

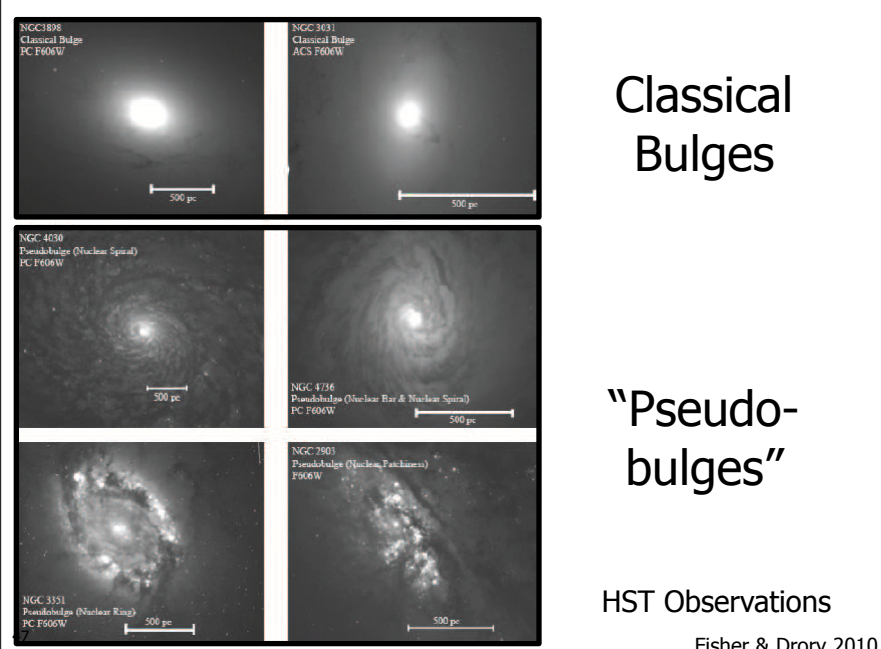
45

## Two Types of Bulges?

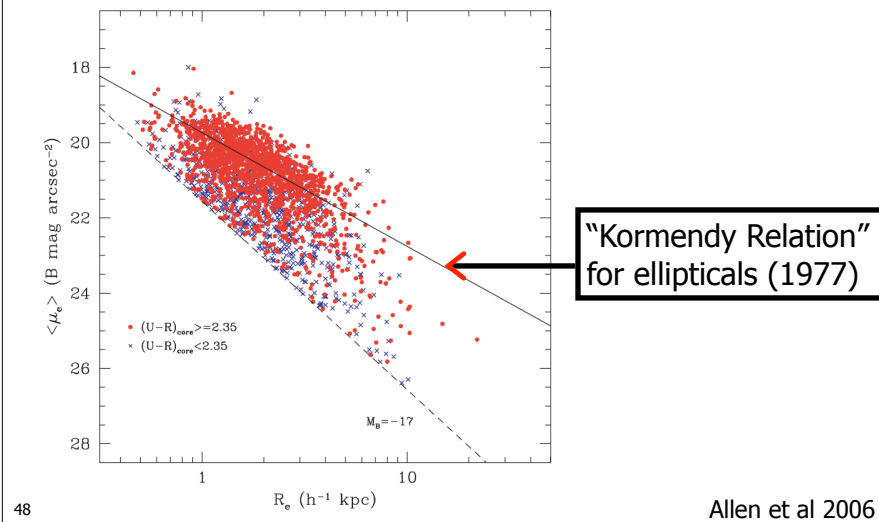


46

Structurally, classical bulges are similar to ellipticals

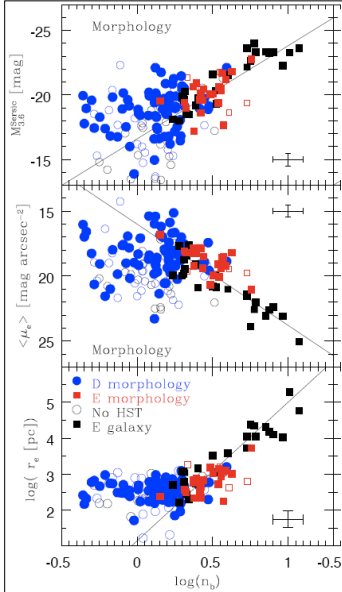


47



48

48



## "Pseudobulges" have $n < 2$ and weak correlations.

Based on decompositions of HST images

We define "bulges" photometrically, as excess light over the inward extrapolation of the surface brightness profile of the outer disk. The region of the galaxy where this excess light dominates the profile is the bulge region. We classify galaxies as having a pseudobulge by their morphology within this bulge region; if the bulge is or contains any of the following features: a nuclear bar, a nuclear spiral, and/or a nuclear ring, then the bulge is called a pseudobulge. Conversely, if the bulge better resembles an elliptical galaxy (relatively featureless isophotes), then the bulge is called a classical bulge. This method is discussed in KK04. The existence/absence of visibly identifiable disk-like structure in a bulge correlates with properties of the bulge and the whole galaxy. The same method is shown to be successful in identifying bulges with higher specific star formation rates (Fisher 2006) and globally bluer galaxies (Drory & Fisher 2007).

Fisher & Drory 2010

FIG. 7.— Correlations of the bulge Sérsic index with (from bottom to top) half-light radius of the bulge (a), average surface brightness within the half-light radius (b), and magnitude of the bulge at  $3.6 \mu\text{m}$  (c). In all panels, pseudobulges are represented by blue circles, classical bulges by red squares, and elliptical galaxies by black squares. Galaxies in the high quality sub-sample are shown as filled symbols whereas galaxies that do not meet criteria for the high-quality data set (see text) are shown as open symbols.

49

## Bulge Formation:

- Primordial Elliptical that accretes a disk? ("classical bulge")
- "Secular" Bulge grows through disk instabilities ("pseudobulge")

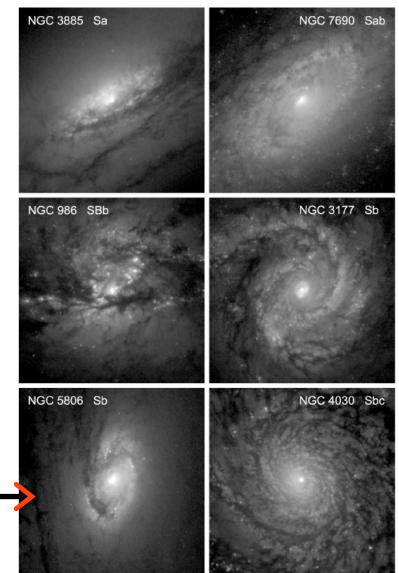


Figure 5. Sa – Sbc galaxies whose "bulges" have disk-like morphology. Each panel shows an  $18'' \times 18''$  region centered on the galaxy nucleus and extracted from HST WFC2 F606W images taken and kindly provided by Carollo et al. (1998). North is up and east is at left. Displayed intensity is proportional to the logarithm of the galaxy surface brightness.

50 See Kormendy & Kennicutt 2005, ARAA

50

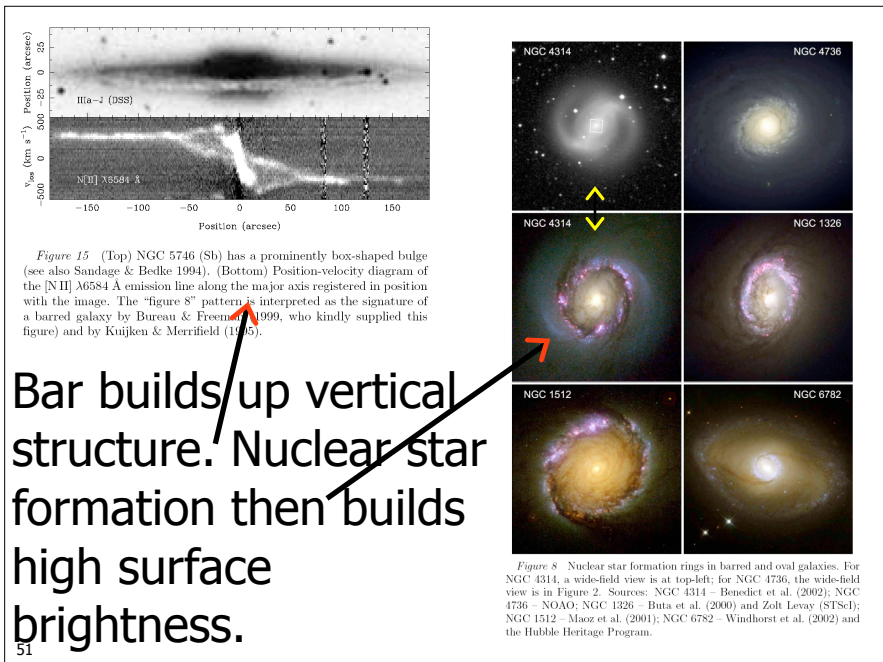


Figure 15. (Top) NGC 5746 (Sb) has a prominently box-shaped bulge (see also Sandage & Bedke 1994). (Bottom) Position-velocity diagram of the [NII]  $\lambda 6584 \text{ \AA}$  emission line along the major axis registered in position with the image. The "figure 8" pattern is interpreted as the signature of a barred galaxy by Bureau & Freeman (1999, who kindly supplied this figure) and by Kuijken & Merrifield (1995).

Bar builds up vertical structure. Nuclear star formation then builds high surface brightness.

51

51